



1 **Landslide susceptibility mapping using fuzzy logic and multi-criteria evaluation**
2 **techniques in the city of Quito, Ecuador**

3
4 Daniela Salcedo, Oswaldo Padilla Almeida, Byron Morales and Theofilos Toulkeridis

5
6 Universidad de las Fuerzas Armadas ESPE, Sangolquí, Ecuador

7
8 dasalcedo@espe.edu.ec, bomorales1@espe.edu.ec, ovpadilla@espe.edu.ec, ttoulkeridis@espe.edu.ec

9
10 **ABSTRACT**

11 Landslides are the most recurrent natural hazards in the Metropolitan District of Quito
12 (DMQ), affecting sometimes lives but extremely frequently and severely the traffic and
13 associated infrastructure. The present research proposes the calculation of the landslide
14 susceptibility cartographic model in the city of Quito and its main highway, the Simón
15 Bolívar avenue, using the Fuzzy logic and multicriteria evaluation techniques in
16 geographic information systems (GIS). Based on the "Today and the past son key to the
17 future" principle, landslides have been located using aerial photographs and field work.
18 Based on the characteristics of historical landslides, photointerpreted and previous
19 studies, the causal factors have been variable such as topography, structural geology,
20 lithology, precipitation, water network, vegetation cover, among others. Each factor has
21 been processed, analyzed and standardized according to its relationship to the occurrence
22 of landslides, by means of a sinusoidal linked function that assigns to each element a



23 degree of correlation [0,1] to the diffuse set. The landslide vulnerability map has been
24 obtained from the combination of causal factors by map algebra, such as weighting
25 techniques that include the hierarchical analysis process (HAP) and the weighted linear
26 line (WLL), whose validation considered the locations of inventoried landslides.
27 According to the susceptibility map, 5% of the direct study area has critical, 19% high,
28 58% average and 18% low sensitivity. The quality of the results has been validated
29 according to their standard error and adjustment value, being 0.216 and 78.4%,
30 respectively.

31

32 **Key words:** Landslide susceptibility map, Fuzzy Logic, GIS, Simón Bolívar Highway.

33

34 INTRODUCCIÓN

35 Landslides constitute one of the most damaging natural hazards in mountainous areas
36 generating human, material and economic losses (Álcantara–Ayala et al, 2006).
37 According to statistics from the Center for Research on the Epidemiology of Disasters
38 (CRED), landslides and other types of mass movement are responsible for 17% of all
39 natural hazard fatalities worldwide (Lacasse et al., 2010), while economic and social
40 losses due to such types of catastrophic events are able to be reduced by a more efficient
41 land use and projection (Rajakumar, et al., 2007). Landslide risk (R) has been usually
42 described as a function of the probability and consequence of landslides (Andersson-
43 Skold et al., 2014)



$$R = \int (P, C_i) \quad (1)$$

Where P is the probability of risk, and C is a vector C_i for all potential consequences. Quantifying potential consequences C_i such as loss of life or damage is difficult because of incomplete or limited historical records that affect population and infrastructure estimates at risk (Grahn and Jaldell, 2017). However, the probability of risk (P) has been analyzed from different evaluation approaches such as qualitative, through geological and geomorphological analysis (Park et al, 2013) and such as quantitative, considering causal factors and probabilistic methods, the same ones that have taken force due to computational and geospatial technological improvements (Bai, et al., 2010). However, the semi-quantitative have been through cause, effect and consequence where instability factors have been selected and weighted according to their relationship with the presence of the event and the occurrence of losses or damages. This has been previously applied within the risk classification system for cut and refill of slopes as well as for natural slopes in future development zones (Koirala and Watkins, 1988; Castellanos Abella and Van Westen, 2007).

The susceptibility maps of landslides have been developed through several methods, of which the most used are the inventory of landslides based on probabilistic techniques, the deterministic as well as the heuristic and statistical techniques (Guzzetti et al., 1999; Chiessi et al., 2016). The first three methods assign weights to a series of causal factors used according to the researcher's experience (Isik, 2009), while statistical analysis considers causal factors in areas with similar environmental conditions to those of past landslides (Park et al., 2013). Nowadays, non-parametric techniques such as cellular



65 automata, Fuzzy logic and artificial neural networks are applied (Falaschi et al., 2009;
66 Pradhan and Lee, 2010; Pradhan, 2013; Saro, et al., 2016).
67 Geographic Information Technology such as Remote Sensors (RS), Geographic
68 Information Systems (GIS) and Global Positioning Systems (GPS) allow the
69 management, assessment and identification of landslide risk. The use of GIS has been
70 positioned because of its ease of collection and analysis of spatial data (Bayes, 2015;
71 Pradhan, 2013). GIS supported by multicriteria decision analysis, such as: weighted
72 average, analytical hierarchy process, weighted linear combination, order among others,
73 are useful procedures for the recognition, evaluation and prognostication of risk by
74 landslides (Feizizadeh & Blaschke, 2013). The most appropriate approach and methods
75 for the evaluation of susceptibility and hazards to landslides have not been defined
76 (Brabb, 1984), their selection depend on the characteristics of the study area both their
77 baseline, historical, developed research and work scale (Hervás et al., 2012)
78 The risk assessment for landslides by means of cartography allows communication with
79 direct involved persons for future impacts and public authorities responsible for risk
80 management and prevention (Andersson-Sköld et al., 2013 Kjellgren, 2013; Andersson-
81 Sköld et al., 2014), allowing the development of effective strategies for stabilization of
82 vulnerable areas, urban planning and implementation of infrastructure (Dahal & Dahal,
83 2017). According to Brabb, (Brabb, 1993), 90% of landslide losses could be avoided if
84 the problem would have been previously recognized prior the catastrophic event
85 (Pardeshi et al., 2013).



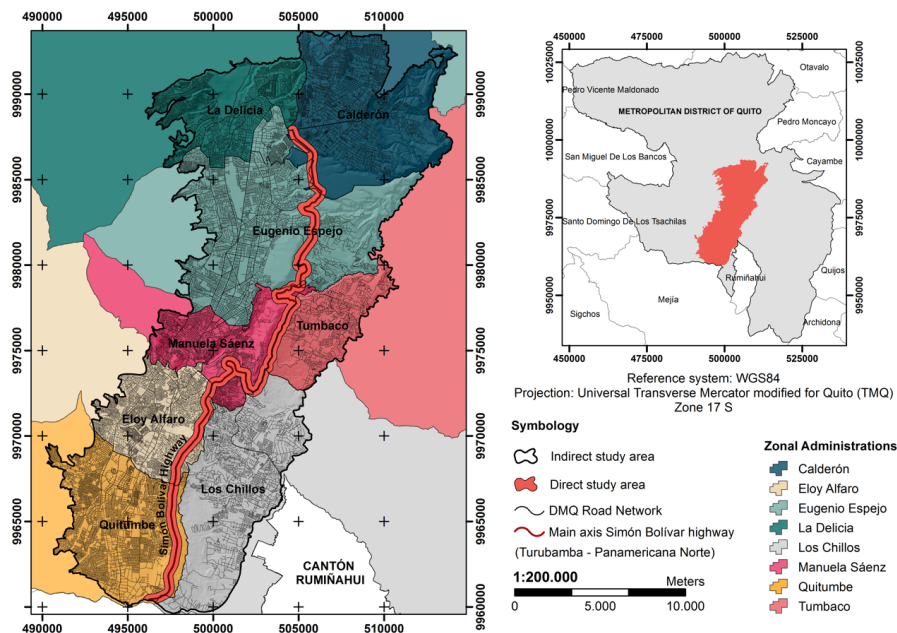
86 Therefore, the main aim of this study has been to generate a cartographic model of
87 susceptibility to landslides of the city of Quito in general and its main highway named
88 Simón Bolívar Avenue, using Fuzzy Logic methodology and multicriteria evaluation in
89 GIS adjusted to historical records that allows the preventive evaluation of susceptible
90 zones in order to avoid human and financial losses, as well as of infrastructure.

91

92 **STUDY AREA**

93 The study area evaluates the susceptibility of the main axis of the Simón Bolívar Avenue,
94 Quito's main highway from its southern end (Turubamba) along with its connection with
95 the Bicentennial Avenue towards its northern end at the Pan-American Highway. In order
96 to validate the results with historical information, we considered an area of indirect
97 influence (AII) with an extension of approximate 393.3 Km², which included the zonal
98 administrations of Los Chillos, Quitumbe, Eloy Alfaro, Manuela Sáenz, Tumbaco,
99 Eugenio Espejo, Calderón and La Delicia, while the area of direct influence (ADI)
100 comprised of some 22.53 Km² covering a radius of 275 m on each side of the main road
101 axis (Fig. 1). The Simón Bolívar Avenue is the main highway of the city of Quito and
102 forms part of its eastern peripheral ring. This highway has been conceived within the
103 mobility plan as a traffic solution when connecting with the northern and southern sectors
104 as well as the valleys bordering the Metropolitan District of Quito (MDQ; 2009; Google
105 Earth Pro, 2017).

106



107
108 **Figure 1.** Location map of the study area

109 Within the ADI, the volcano - sedimentary fill comprises deposits of lava, agglomerates,
110 tuffs, volcanic ash, layers of pumice and undifferentiated sediments being part of the
111 geological formations such Machángara (Pleistocene) and Chiche as well as primary and
112 colluvial volcanic deposits that have been generated during the Holocene (INIGEMM,
113 1978-1980). The topography varies between 1915 and 3380 meters above sea level
114 (m.a.s.l.). The Machángara river crosses the road artery in the sector of Guápulo, which
115 raised from the tributaries: Ortega, Shanshayacu, Rio Grande and Capulí or Machángara,
116 conformed by 22.5 km and bordered by very steep slopes, is the main stream and more
117 (EPMAPS), along with the Monjas River of the DMQ (El Comercio, 2015a), where
118 76.3% of urban wastewater flows from the south, center and north of the city to the level



119 of the Guayasamín tunnel without any type of previous treatment (Moreano, 2010),
120 having an organic load with 80% of domestic and 20% industrial origin, respectively
121 (Reinoso Chisaguano, 2015). Soil is commonly used in infrastructure and the vegetation
122 cover is made up of both wet and dry shrubs and broadleaf cultivated vegetation
123 (Secretaría de Seguridad y Gobernabilidad del DMQ, 2015). The maximum precipitation
124 is given to the southern sector of the city and decreasing towards the north (Secretaría de
125 Seguridad y Gobernabilidad del DMQ, 2015).

126 Simón Bolívar Avenue is the first roadway with the highest vehicular traffic of the DMQ.
127 Through there, 74,469 vehicles pass through (EPMOP) (El Comercio, 2015b).
128 However, there are six areas prone to landslides in the winter season (El Comercio,
129 2012). Its implementation in mountainous area, proximity to natural channels, deficient
130 or absent channeling of rainwater, human settlements, anti-technical discharges of
131 sewage and deforestation have influenced the frequency of landslides especially in the
132 rainy winter season where their constant work of soil removal and maintenance represent
133 a high public investment in rehabilitation and reconstruction, incurring high levels of
134 congestion, human losses, and material, affecting infrastructure and commercial sectors
135 (Toulkeridis et al., 2016).

136 In 2011, the road has been completely disabled for two weeks due to the landslide of
137 49,700 m³ of land that registered 5 fatalities and 120 evacuated in the sector of Forest IV,
138 (El Comercio, 2011), while the Municipality invested 636,478 dollars in stabilization
139 works (Prensa Alcaldía de Quito, 2011). Considering the vulnerability of the road, the
140 Metropolitan Public Company for Mobility and Public Works (EPMOP) has taken



141 precautionary measures through works of cleaning both the vegetation layer and ditches
142 of coronation and tracks, slope profiling and implementation of complementary works
143 for water eviction, in sectors such as El Madrigal, San Isidro de Puengasí,
144 Chaquishahuaycu ravine, among others, where a variety of slope stabilization works have
145 been performed (El Telégrafo, 2013).

146 In 2016, EPMMOP handled 28 landslides along Avenida Simón Bolívar, of which 11
147 have been in Guápulo and the remaining in the sectors Alma Lojana, Santa Rosa,
148 Monteolivo, Las Bromelias, Miravalle 4, Oswaldo Guayasamín, Chaquishahuaycu
149 Creek, Zambiza, Algeria Alta, El Troje, Llano Chico, Granados, Guajaló, San Francisco,
150 La Forestal and Nuns (EPMMOP).

151 In 2017, the DMQ recorded the highest precipitation levels of the last 30 years (Prensa
152 Alcaldía de Quito, 2017), where main roads such as Av. Velasco Ibarra and Av. Simón
153 Bolívar were heavily affected. Between October 2016 and May of 2017, Quito attended
154 965 emergencies, of which 443 have been landslides (El Universo, 2017). 14.7 million
155 dollars have been allocated to the prevention and response plan for rainy season, plus
156 further two million US Dollars from the emergency fund, where 1,870 officials have been
157 mobilized for disaster prevention and care (Alcaldía de Quito, 2017, La Hora, 2017), a
158 management that has been recurrent in previous years.

159

160 MATERIALS AND METHODS

161 The areas prone to landslides have been determined using a heuristic method, a
162 qualitative analysis where a series of factors related to the occurrence of landslides is



163 selected, hierarchized and weighed. The susceptibility of these landslides has been solved
164 through decision tools applied in GIS (Andocilla et al, 2012; Ciampalini et al., 2016;
165 Jaramillo et al., 2018; Zafrir et al., 2018) due to the ease of handling spatial information,
166 versatility of representation and quality of results.
167 The applied methodology has been based on the principle "Today and the past are keys
168 to the future" (REF), considering that: (1) Future landslides will have the same
169 geological, geomorphological and water factors as those already in the past or in nearby
170 previously studied areas; and (2) Causal factors will be represented by spatial data
171 contained in a GIS database that will allow diffuse overlap (Maryam, 2011). The causal
172 factors have been standardized using a membership function according to the relationship
173 between the dependent variable (presence or absence of landslides) and independent
174 variables (landslides / causal factors). The obtained results from each map factor have
175 been weighted by hierarchical analysis (AHP) according to their relevancy with the
176 occurrence of landslides.

177

178 **DETERMINATION OF CAUSAL FACTORS**

179 The causal or instability factors have been divided into conditioning factors and triggers,
180 the former depending on the characteristics of the area such as topography, geology,
181 lithology, soil type, drainage and vegetation cover (Dahal & Dahal, 2017). The second
182 increase the probability of occurrence, being of natural origin such as earthquakes,
183 precipitation intensity and natural or anthropic erosion due to land use and construction
184 operations (Singh, 2010). Both of them vary significantly from one region to another



185 (Pardeshi, Autade, & Pardeshi, 2013), so it has been fundamental to determine them by
186 means of a retrospective analysis. According to geomorphological factors, slope, climate
187 and human intervention play an important role (Biju Abraham & Shaji, 2013).
188 According to the National Institute of Statistics and Censuses (INEC), rapid urbanization
189 within the DMQ has increased settlements in inadequate areas such as slopes or edges of
190 rivers and streams that produce vulnerable sectors especially in winter (Sepúlveda &
191 Petley, 2015; Secretaría de Seguridad y Gobernabilidad, 2015). At the same time the
192 implementation of roads in mountainous regions has generated problems of instability
193 that geologists and civil engineers have been aware of (Silvers and Griffiths, 2006;
194 Fookes et al., 1985; Transport Research Laboratory, 1997)
195 The scarce vegetation cover of steep slopes has been affected by forest fires, being one
196 of the most frequent phenomena of the DMQ, where approximately nine events on the
197 Simón Bolívar Avenue and surrounding areas have been registered in 2016 (Secretaria
198 de Gestión de Riesgos, 2016; Cantuña et al., 2017).
199 Considering the historical record of landslides on Avenida Simón Bolívar in sectors such
200 as Forestal IV (2011), Buenos Aires (2015), detour of Granados (2016 and 2017), El
201 Troje (2017), Monteolivo (2017), Puengasí 2017), La Forestal (2017), as well as causal
202 factors exposed in studies developed by the Municipality, projects in the Monjas -
203 Ferroviaria - La Magdalena - Itchimbia area and the zonal administration Eugenio Espejo
204 (Andocilla et al, 2012; Jaramillo et al., 2018; Zafirir et al., 2018). Generating or causal
205 factors have been considered to be the topography, geology, lithology, vegetation cover,
206 precipitation, water network and the main accessibility.



207

208 **Standardization, weighting and evaluation**

209 As each factor has a different scale of measurement and cartographic representation
 210 (vector or raster) to perform a multicriteria analysis, therefore the input layers need to be
 211 standardized from their original values to values in a range of 0 to 1 according to the
 212 normalization formula (Equation (2)). The standardization has been performed by Fuzzy
 213 logic in order to assign to each element a membership value according to the degree of
 214 membership in the set. The membership function is of sinusoidal type whose value
 215 oscillates between 0 and 1 by the use of sine curves (Fig. 2) and cosine (Fig. 3) in a range
 216 of 0 to 90 ° ($\pi / 2$ radians), its occupation will depend on the relationship between the
 217 analyzed variable and the probability of landslides (Zafrir et al., 2015). The limits of the
 218 function correspond to the maximum and minimum values of each factor taking into
 219 account that all values represent a level of risk.

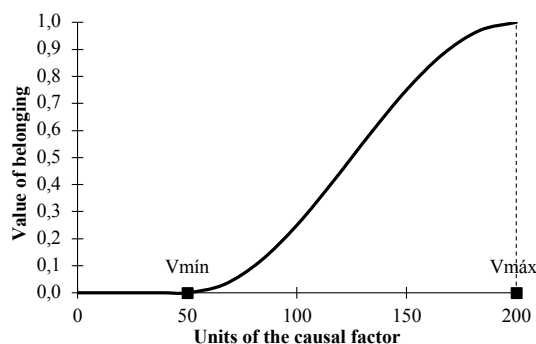
Normalization:

$$N = \frac{V_o - V_{min}}{V_{max} - V_{min}} \quad (1)$$

220 Where: V_o : Original value; V_{min} : Minimum value and, V_{max} : Maximum Value.

221 Directly proportional (2nd Case):

$$\mu_A(V_o) = \sin\left(\frac{\pi}{2} \times \frac{V_o - V_{min}}{V_{max} - V_{min}}\right) \quad 0 \leq \mu_A(V_o) \leq 1 \quad (2)$$

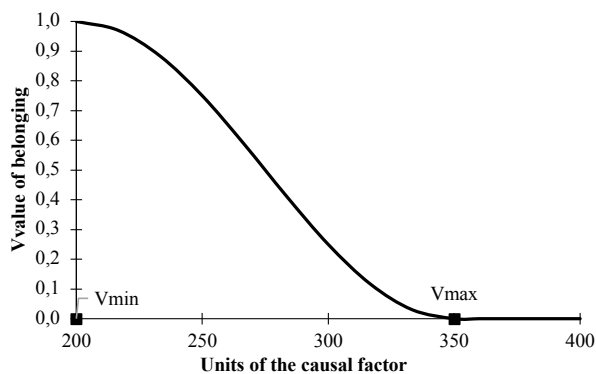


222

223 **Figure 2.** Sine curve belonging function from 0 to $\pi/2$ radians (Zafrir et al., 2015)

224 Inverse proportional (3rd Case):

$$\mu_A(V_o) = \cos\left(\frac{\pi}{2} \times \frac{V_o - V_{min}}{V_{max} - V_{min}}\right) \quad 0 \leq \mu_A(V_o) \leq 1 \quad (3)$$



225

226 **Figure 3.** Curve belonging property Cosine range from 0 to $\pi/2$ radians (Zafrir et al., 2015)

227 Where $\mu_A(V_o) = 1$, si V_o belongs entirely to the set, $\mu_A(V_o) = 0$ si V_o does not belong to the
 228 set and $0 < \mu_A(V_o) < 1$ if V_o is partially in the set.

229 **Table 1.** Functions of belonging to each factor. The Sine and Cosine belonging functions have

230 been evaluated from 0° to 90°

Factor	Relation parameter between:	Standardization Method: Fuzzy Logic
--------	--------------------------------	--



	Factor / Landslide	Sinusoidal belonging function
Slope	Directly proportional: The greater the value of the factor, the greater susceptibility to landslides	Sinus
Precipitation		Sinus
Plant cover		Sinus
Distance to communication routes	Inversely proportional: The lower the value of the factor, the greater susceptibility to landslides	Cosine
Distance to water resources		Cosine
Distance to geological faults		Cosine
Rock hardness		Cosine

231

232 RESULTS AND DISCUSSION

233 The landslides have been located and inventoried through aerial photographs taken in
 234 2011 by the IGM, Digital Terrain Model and Ortho-mosaic scale 1: 1000 DMQ, provided
 235 by the Ministry of agriculture, livestock, aquaculture and fisheries based on the Project
 236 National System of Information and Management of Rural Lands and Technological
 237 Infrastructure (SIGTIERRAS), considering areas of rupture, bare soil and other typical
 238 geomorphological characteristics. The map of the sliding inventory has been used to
 239 evaluate the spatial distribution of landslides and to determine their triggering factors in
 240 the study area (Pradhan, 2013). A total of 45 landslides have been identified at Avenida
 241 Simón Bolívar, through photointerpretation and field tests with the use of a Global
 242 Positioning System (GPS) with a precision of 4 m.

243

244 Slope Map

245 The slope map has been generated from the scale curves 1: 5000 and MDT. Altitudes
 246 vary from 1915 m to 3380 m, where the maximum slope has been of 88.68°, and the
 247 minimum corresponds to flat areas with 0°.



248

249 **b) Vegetation cover map**

250 The vegetation cover map has been weighted considering similar studies within DMQ

251 (Loarte Merino, 2013; Zafrir et al., 2015), considering a susceptibility range from 1

252 (Low) to 5 (Very High).

253 **Table 2.** Weighting of plant cover based on Loarte Merino (2013)

Level I	Level II	Level III	Weighting
Forests and semi-natural areas	Planted vegetation of conifers	Pines and Cypress	1
	Planted vegetation of broadleaves	Grown Eucalyptus Young and regeneration Eucalyptus	1
	Vegetation in natural regeneration	Secondary forest Brush in regeneration Cork with trees Cork with bushes	1
Natural vegetation	Wet grasslands	Upper montane and montane paramo grassland Upper montane subhumid paramo grassland	2
	Dry grasslands	Interandean montane saxicolous vegetation	2
	Rainforests	Evergreen northern Andean forests High Andean paramo dwarf shrubland North Andean montane pluvial forest North Andean foothill pluvial forest Low montane seasonal evergreen forests	1
	Dry forests	Interandean dry forest Xeric riparian montane vegetation	1
	Humid bushes	High-andean shrubby paramo Northern Andes montane shrubland	2
	Dry bushes	Interandean dry bushes	2
Agricultural areas	Crops	Short cycle crops Semi-permanent and permanent crops Soils in preparation.	4
		Cultivated pasture	5
	Pastures	Natural pasture	3
Storage Areas	Infrastructure	Airports Buildings Greenhouses	2
Open space	Bare soils of natural origin	Beaches	5
		Glaciers	4
		Rock	4



	Bare soils of anthropogenic origin	Eroded soils Quarries	5
Waters capes	Water in natural channels	Rivers	3
	Water in artificial channels	Reservoirs	1

254

255 c) Precipitation map

256 The annual precipitation records for 25 years (1991-2015) have been provided by the
 257 National Institute of Meteorology and Hydrology (INAMHI), whose nearby stations
 258 have been listed in Table 3. The estimation of precipitation in stations with incomplete
 259 statistics have been performed using the average ratio completion method or the normal
 260 ratio (Equation (5)), recommended for mountain areas where the precipitation of nearby
 261 stations generally differ by more than 10%, by which the relationship between the station
 262 "x" and its nearby stations in a period has been considered (UNESCO - ROSTALC,
 263 1982).

$$P_x = \frac{1}{n} \left[\left(\frac{N_x}{N_1} \right) P_1 + \left(\frac{N_x}{N_2} \right) P_2 + \dots + \left(\frac{N_x}{N_n} \right) P_n \right] \quad (4)$$

264 Where n represents number of rainfall stations with continuous recorded data close to
 265 the station "x", which will be completed in its registry; P_x represents precipitation of the
 266 station "x" during the time period to be completed; P_1 to P_n shall be the precipitation of
 267 nearby stations during the time period to be completed; N_x represents the annual average
 268 season precipitation of station "x"; N_1 to N_n represents the annual average precipitation
 269 of the stations nearby (Monsalve, 2009).



The homogeneity of the data has been estimated by the average ratio completion method or the normal ratio being verified by double mass analysis, which consisted of constructing a cumulative double curve that relates the cumulative annual precipitation totals of the station “x” and its near station (Monsalve, 2009). The obtained correlation coefficients from the double mass curve for all the stations have been close to one, which evidenced the homogeneity of the data. The results have been verified by means of test of streaks, where their homogeneity has been confirmed. Table 3 illustrates the results of annual average precipitation of each station used for the mapping of Isoyetas.

Table 3. Results of the annual average precipitation

Code	Station	Coordinates		Altitude	Annual average precipitation
		Latitude	Longitude	z (m)	(mm)
M0002	LA TOLA	0° 13' 54.0" S	78° 22' 13" W	2480	844.02
M0003	IZOBAMBA	0° 21' 57.0" S	78° 33' 18" W	3058	1467.21
M0335	LA CHORRERA	0° 12' 06.0" S	78° 32' 06" W	3165	1481.33
M0343	EL QUINCHE-PICHINCHA	0° 06' 31.2" S	78° 17' 53" W	2605	336.86
M0345	CALDERON	0° 05' 54.0" S	78° 25' 15" W	2645	546.00
M0353	RUMIPAMBA-PICHINCHA	0° 25' 51.8" S	78° 25' 6.8" W	2940	1853.86
M0354	SAN JUAN-PICHINCHA (CHILLOG.)	0° 17' 30.3" S	78° 37' 27.6" W	3440	1917.63
M0358	CALACALÍ INAMHI	0° 00' 05.9" N	78° 30' 46.3" W	2810	779.16
M0361	NONO	0° 02' 19.2" S	78° 33' 50.8" W	2710	946.81

d) Lithology Map

The lithology map has been weighted by a numerical scale where 1 represents the highest vulnerability and 6 the lowest, according to field experience. In flat areas, the effect of lithology has been reduced due to the absence of landslide vulnerability.



Table 4. Weighting of the Lithology

Lithology	Weighting
Agglomerate, undifferentiated lava	4
Andesites	5
Cangahua on colluvial deposits	3
Cangahua on sedimentary deposits Chichi Formation	3
Cangahua on sedimentary deposits of Atacazo volcano	3
Cangahua on volcanic deposits of Pichincha volcano	3
Cangahua on volcanic deposits of Ilaló volcano	3
Cangahua on undifferentiated volcanic deposits	3
Cangahua on volcanic – sedimentary deposits of Machángara	3
Ashes	3
Ashes with lapilli pumices	3
Natural or artificial water channel	6
Alluvial Reservoir	6
Colluvial Deposit	1,50
Lake deposits of ash	6
Lahar deposits	4
Landslide or collapse material	1
Natural or artificial water channel	6
Fillings	1,75
Artificial fillings	1,75
Sediments of Chichi Formation	1
Undifferentiated Terrace	6
Terrace, Gravel	1,50
Terrace, Cangahua type	2
Undifferentiated volcanic deposits	1,50
Undifferentiated volcanic – sedimentary deposits	1
Volcanic deposits of Guayllabamba	1
Volcanic – sedimentary deposits of Machángara	2
Volcanic – sedimentary deposits of San Miguel	1

e) Other maps

The geological, hydric and road parameters have been analyzed by proximity using the "Euclidean Distance" tool (ArcGIS), distance from each cell in the raster to the nearest source (geological fault, river and road).

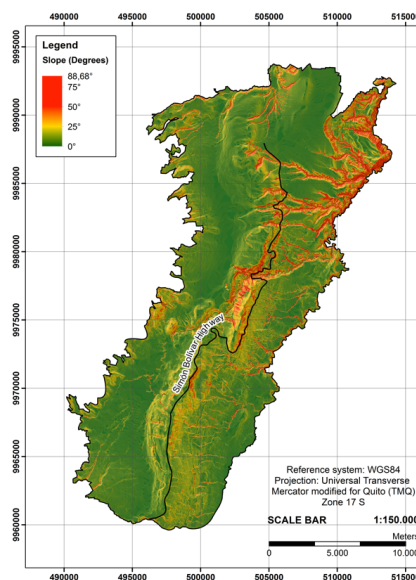


Figure 4. Slope map

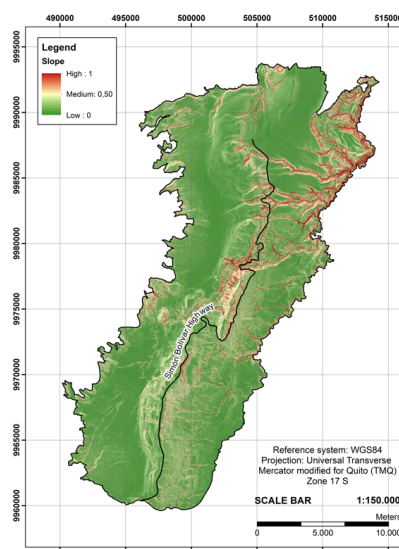


Figure 5. Normalized slope map

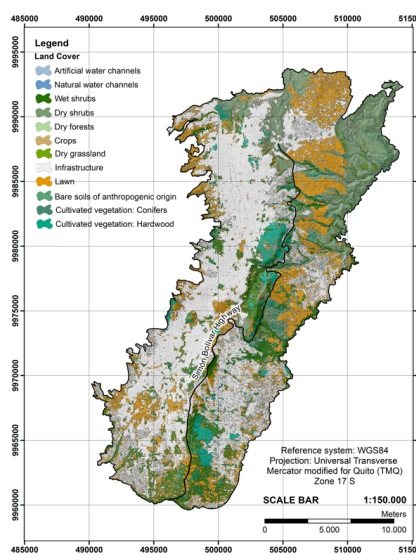


Figure 6. Map of land cover

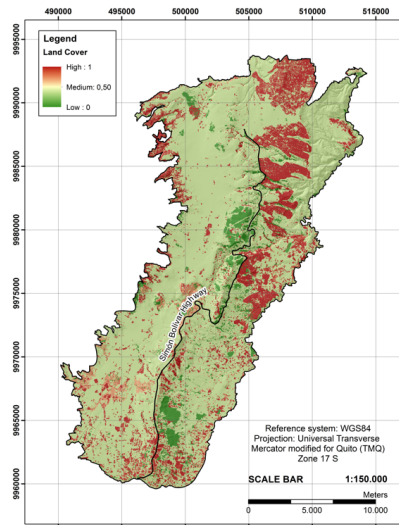


Figure 7. Normalized land cover

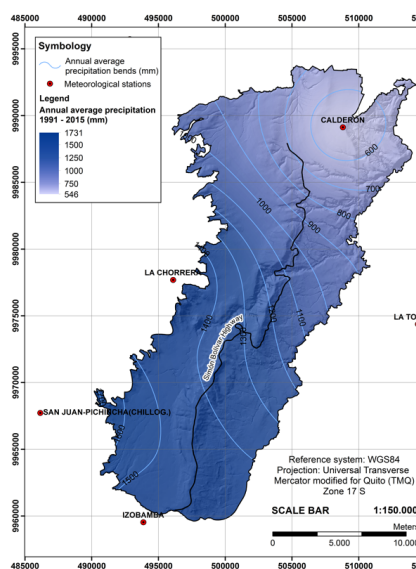


Figure 8. Annual average precipitation bends

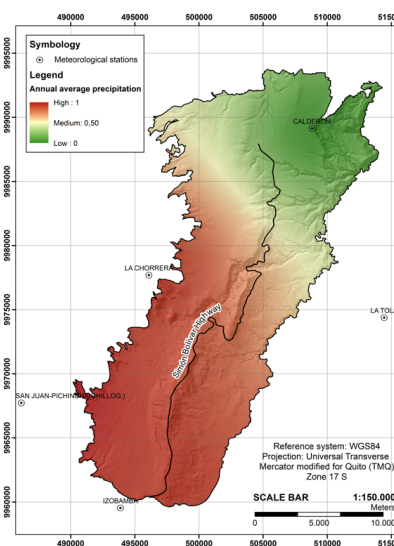


Figure 9. Normalized precipitation bends

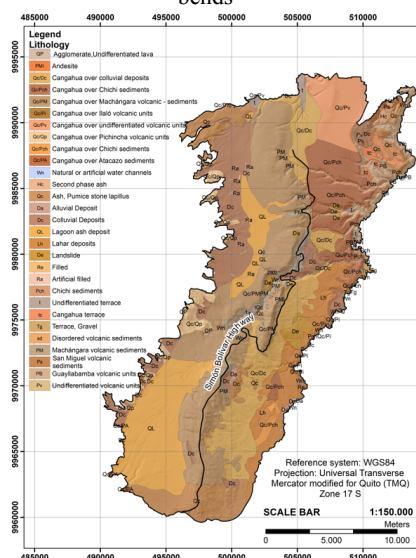


Figure 10. Lithology map

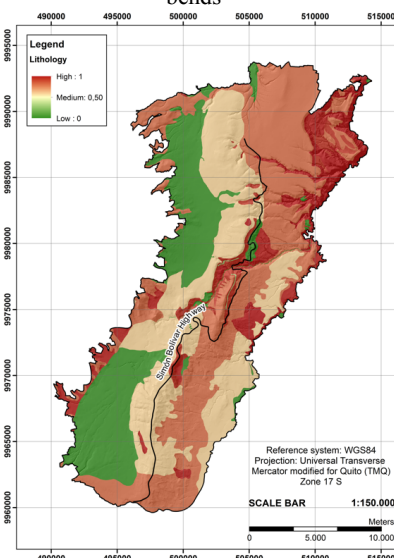


Figure 11. Normalized lithology map

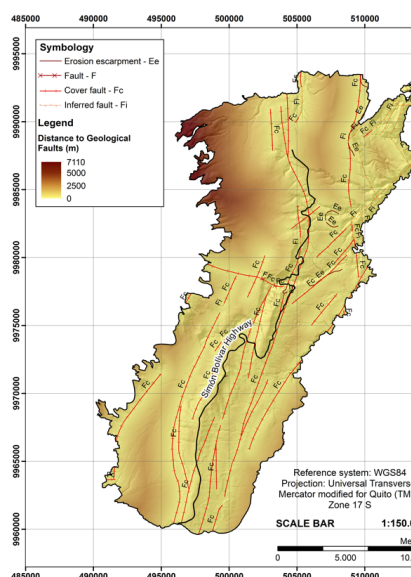


Figure 12. Map with distance of geological faults

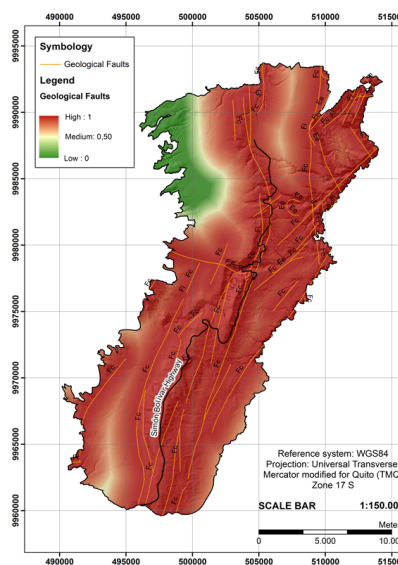


Figure 13. Map with normalized distance of geological faults

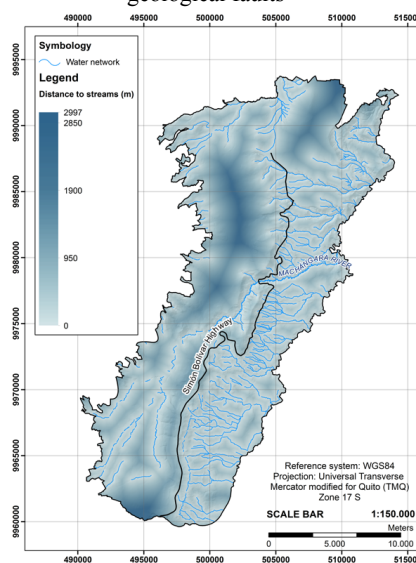


Figure 14. Map with distance to streams

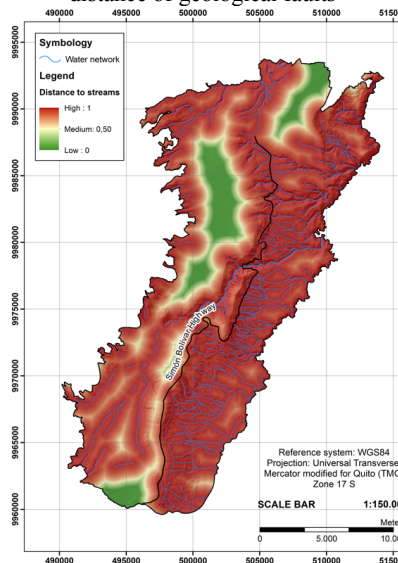


Figure 15. Normalized distance to streams

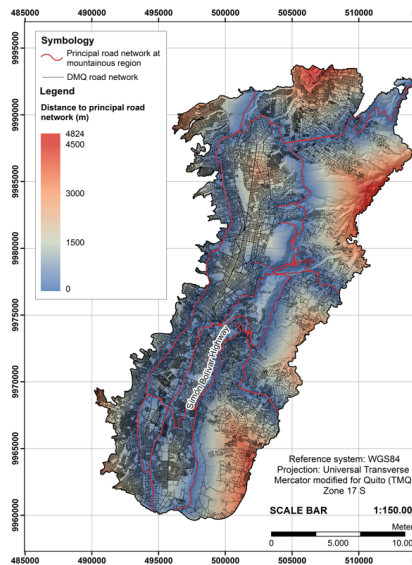


Figure 16. Map with distance to road network

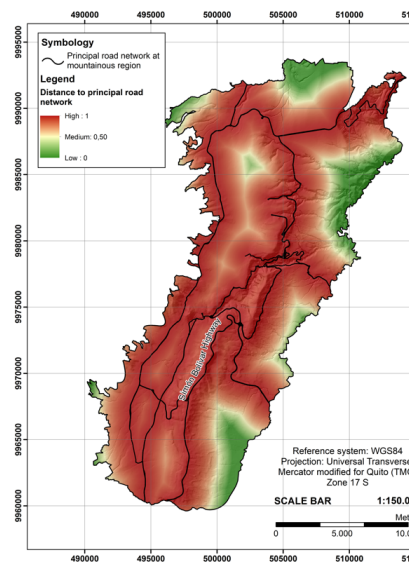


Figure 17. Map with normalized distance to road network

f) Map of susceptibility to landslides through the Hierarchical Analysis Method (AHP)

The matrix of AHP considers three principles: decomposition, comparative judgment and synthesis of priorities (Malczewski, 1996), through which the problem (and its weights) is decomposed in a hierarchical structure, whose weighting depends on the comparison of criteria by pairs and the multiplication between the respective hierarchical levels (Castellanos Abella & Van Westen, 2007). Assigned values range from ("much less important than"); 1 ("equally important than") and, 9 ("much more important than") (Saaty, 1980, Eastman, 2012).



302

Table 5. Hierarchical analysis of causal factors

	(1)	(2)	(3)	(4)	(5)	(6)	(7)	Weighting
(1) Slope	1	3	9	2	8	7	6	0,379
(2) Precipitation	1/3	1	7	1/2	6	3	2	0,159
(3) Plant cover	1/9	1/7	1	1/8	1/2	1/3	1/6	0,024
(4) Lithology	1/2	2	8	1	7	6	3	0,246
(5) Road distance	1/8	1/6	2	1/7	1	1/2	1/3	0,036
(6) River distance	1/7	1/3	3	1/6	2	1	1/3	0,054
(7) Geol. fault distance	1/6	1/2	6	1/3	3	3	1	0,102

303 *CR: 0,030

304 **Weighted linear sum**

305 The susceptibility map has been the result of the combination of causal factors with their
 306 respective weights obtained by AHP as shown in Equation (6)

$$I = \sum_{j=1}^n W_j \times x_{ij} \quad (5)$$

307 Where: I : Susceptibility index, W_j : factor weight j , x_{ij} : normalized value of each map
 308 and n : number of factors. Resulting in:

$$f_{(x)} = 0,379 x_1 + 0,246 x_2 + 0,159 x_3 + 0,102 x_4 + 0,054 x_5 + 0,036 x_6 + 0,024 x_7 \quad (6)$$

309 Where: x_1 : Pending; x_2 : Lithology; x_3 : Precipitation; x_4 : Distance to geological faults;
 310 x_5 : Distance to rivers; x_6 : Distance to roads y, x_7 : Vegetation cover.

311

312 **Model Adjustment**

$$N = Value_{Measured} - Value_{Calculated} \quad (7)$$



$$N = 1 - Y$$

$$N = 1 - 0,1620 \quad (8)$$

$$N = 0,838$$

Where: N : Adjustment; $Value_{Measured}$: 1 or value of the sample points and,
 $Value_{Calculated}$: standard deviation of the resulting model.

Thus, the level of slip irrigation has been classified according to Anbalagan (1992), based
 on the model of Fuzzy logic obtained in a range of 0 to 1 (Maryam, 2011) and represented
 in color scales (Table 6).

Table 6. Slip susceptibility zonation according to the diffuse output membership functions.

Zone	Fuzzy belonging function	Description level of susceptibility	Color of scales
I	< 0.1	None	Dark green
II	- 0.40	Low	Light green
III	0.40 – 0.60	Medium	Yellow
IV	0.60 – 0.75	High	Orange
V	> 0.75	Critical	Red

The obtained susceptibility map from the combination of Fuzzy methodology and
 multicriteria evaluation yielded a standard error of 0.1620 with an adjustment value of
 83.8%. Where 2% of AEI has critical susceptibility, 10% high, 37% average, 49% low
 and 2% nil. Within the AED, 5% have critical susceptibility, 19% high, 58% average and
 18% low. The obtained results have been in accordance with the spatial distribution of
 landslides, together with historical records in areas such as La Ferroviaria, Guápulo,
 Oswaldo Guayasamín, Granados Connection, among others (Fig. 18). The new
 vulnerability map has a more detailed aspect of all used parameters when compared with
 the existing map of the municipality of Quito (Fig. 19).

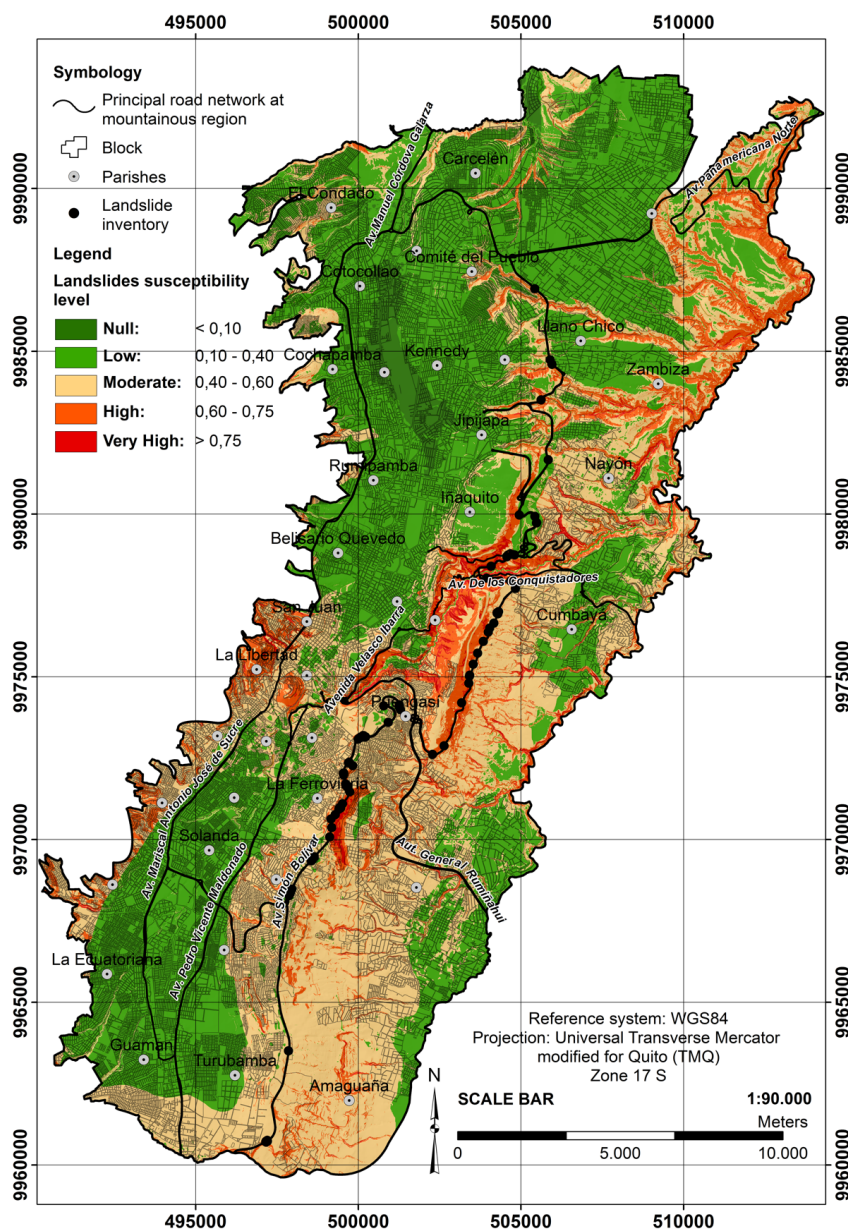


Figure 18. Map of susceptibility to landslides derived from the AHP method.

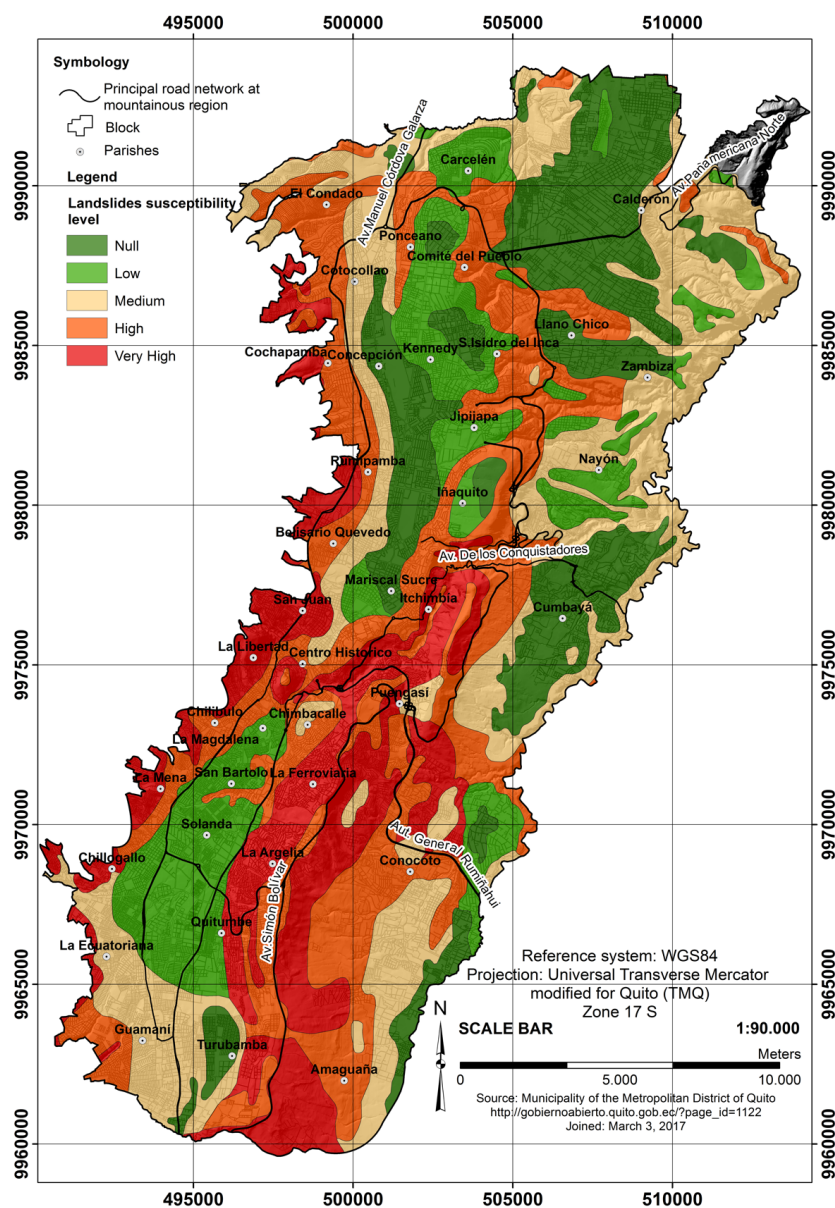


Figure 19. Previously existing map of the susceptibility to landslides from the municipality of Quito.



335 CONCLUSIONS AND RECOMMENDATIONS

336 The Simón Bolívar Avenue has a medium to high level of susceptibility to landslides,
337 where the most critical sectors are located in the parishes such as La Ferroviaria, Puengasí
338 and Itchimbia. A preventive analysis of the area certainly will be more economical than
339 the implementation of corrective measures once the event has been triggered.

340 Topography and geology have been the factors that mainly defined the level of
341 susceptibility as they condition the effect of detonators such as precipitation and
342 anthropic intervention.

343 The parameters and methodology selected for the study area have been considered
344 adequate and coincide with the factors established in the field.

345 The cartographic models of susceptibility to landslides have been useful tools for urban
346 planning and implementation of strategic infrastructure such as road corridors and allow
347 to locate new vulnerable areas beyond the historically recognized. Simultaneously they
348 constitute the baseline for developing models for geotechnical and seismic zoning within
349 the DMQ.

350 The fuzzy methodology combined with multicriteria analysis would have a better
351 correlation with historical data and the spatial distribution of inventoried slides, if the
352 information base of each factor provided by the competent entities would have been
353 updated, validated and at scales of greater precision.

354 Social parameters such as land use, evolution of the urban spot in illegally constituted
355 areas and implementation of strategic infrastructure at the edge of slopes should be
356 included within the causal factors. The inventory of resources affected and at potential



357 risk through multitemporal analysis would make it easier to estimate the human and
 358 economic losses that the landslides have generated and could affect the public and private
 359 sector.

360

361 REFERENCES

362 Agencia Pública de Noticias Quito (2011). Última Fase Para Estabilizar Talud En La
 363 Forestal.

364 http://www.noticiasquito.gob.ec/index.php?module=Noticias&func=news_user_vie
 365 [w&id=4730&umt=%DAltima%20fase%20para%20estabilizar%20talud%20en%20](http://www.noticiasquito.gob.ec/index.php?module=Noticias&func=news_user_vie)
 366 [La%20Forestal.](http://www.noticiasquito.gob.ec/index.php?module=Noticias&func=news_user_vie)

367 Agencia Pública de Noticias Quito (2017). Alcalde Rodas Declaró En Emergencia Al
 368 Distrito Metropolitano Por Fuerte Invierno.
 369 http://www.noticiasquito.gob.ec/index.php?module=Noticias&func=news_user_vie
 370 [w&id=24699&umt=Alcalde%20Rodas%20declar%F3%20en%20emergencia%20al](http://www.noticiasquito.gob.ec/index.php?module=Noticias&func=news_user_vie)
 371 [%20Distrito%20Metropolitano%20por%20.](http://www.noticiasquito.gob.ec/index.php?module=Noticias&func=news_user_vie)

372 Álcantara-Ayala, I., Esteban-Chavez, O. and Parrot, J. (2006). Landsliding related to
 373 land- cover change: A diachronic analysis of hillslope instability distribution in the
 374 Sierra Norte, Puebla, Mexico. CATENA, 65, 152 - 165.

375 Anbalagan, R. (1992). Landslide hazard evaluation and zonation mapping in
 376 mountainous terrain. Eng.Geol, 32(4), 269-277

377 Andersson-Sköld, Y., Bergman, R., Johansson, M., Persson, E. and Nyberg, L. (2013).
 378 Landslide risk management—A brief overview and example from Sweden of current
 379 situation and climate change. International Journal of Disaster Risk Reduction, 3, 44
 380 - 61.

381 Andersson-Skold, Y., Falemo, S. and Trembaly, M. (2014). Development of
 382 methodology for quantitative landslide risk assessment-Example Gota river valley.
 383 Natural Science, 6, 130 - 143.



- 384 Andocilla, L., Padilla, O. and Cruz, M. (2012). Implementación del algoritmo de lógica
 385 Fuzzy aplicado a la determinación del grado de susceptibilidad a deslizamientos en el
 386 área Monjas - Ferroviaria - La Magdalena - Itchimbia del Distrito Metropolitano de
 387 Quito. *Revista Geoespacial*, 9, 12 - 29.
- 388 Bai, S.-B., Wang, J., Lü, G.-N., Zhou, P.-G., Hou, S.-S. and Xu, S.-N. (2010). GIS -
 389 based logistic regression for landslide susceptibility mapping of the Zhongxian
 390 segment in the Three Gorges area, China. *Geomorphology*, 115, 23 – 31.
- 391 Bayes, A. (2015). Landslide susceptibility mapping using multi-criteria evaluation
 392 techniques in Chittagong Metropolitan Area, Bangladesh. *Landslides*, 12, 1077 –
 393 1095.
- 394 Biju Abraham, P. and Shaji, E. (2013). Landslide hazard zonation in and around
 395 Thodupuzha-Idukki-Munnar road, Idukki district, Kerala: A geospatial approach.
 396 *Journal of the Geological Society of India*, 82, 649–656. doi:10.1007/s12594-013-
 397 0203-7
- 398 Biju Abraham, P. and Shaji, E. (2013). Landslide hazard zonation in and around
 399 Thodupuzha-Idukki-Munnar road, Idukki district, Kerala: A geospatial approach.
 400 *Journal of the Geological Society of India*, 82, 649 – 656.
- 401 Brabb, E. (1984). Innovative approaches to landslide hazard and risk mapping. 4th
 402 International Symposium on Landslides, 307 - 323.
- 403 Brabb, E. (1993). Proposal for worldwide landslide hazard maps. Proceedings of 7th
 404 International Conference and field workshop on landslide in Czech and Slovak
 405 Republics, 15 – 27.
- 406 Cantuña, J. G., Bastidas, D., Solórzano, S. and Clairand, J. M. (2017). Design and
 407 implementation of a Wireless Sensor Network to detect forest fires. 2017 4th
 408 International Conference on eDemocracy and eGovernment, ICEDEG 201729 June
 409 2017, Article number 7962508, Pages 15-21
- 410 Castellanos Abella, E. and Van Westen, C. J. (2007). Generation of a landslide risk index
 411 map for Cuba using spatial multi - criteria evaluation. *Landslides*, 4, 311 – 325.



- 412 Chiessi, V., Toti, S. and Vitale, V. (2016). Landslide susceptibility assessment using
 413 conditional analysis and rare events logistics regression: A case - Study in Antrodoco
 414 Area (Rieti, Italy). *Journal of Geoscience and Environment Protection*, 4, 12, 1 - 21.
- 415 Ciampalini, A., Raspini, F., Bianchini, S., Lagomarsino, D. and Moretti, S. (2016). A
 416 landslide susceptibility map of the Messina Province (Sicily, Italy). *Landslides and*
 417 *Engineered Slopes. Experience, Theory and Practice*, 1, 657 – 661.
- 418 Dahal, B. K. and Dahal, R. K. (2017). Landslide hazard map: tool for optimization of
 419 low-cost mitigation. *Geoenvironmental Disasters*, 4(1), 8 doi:10.1186/s40677-017-
 420 0071-3
- 421 Distrito Metropolitano de Quito. (2009). Plan Maestro De Movilidad Para El Distrito
 422 Metropolitano De Quito: 2009-2025. Quito, Ecuador: 119pp
- 423 Eastman, J. R. (2012). The IDRISI Selva Tutorial Manual Version 17. Clark Labs. Clark
 424 University: 354pp
- 425 El Comercio (2011). Estudios En La Forestal No Terminan.
 426 <http://www.elcomercio.com/actualidad/quito/estudios-forestal-no-terminan.html>
- 427 El Comercio (2015a). La mayor contaminación en ríos y quebradas está en 8 sitios del
 428 sur. [http://www.elcomercio.com/actualidad/quito-contaminacion-rios-aguas-](http://www.elcomercio.com/actualidad/quito-contaminacion-rios-aguas-residuales.html)
 429 [residuales.html](http://www.elcomercio.com/actualidad/quito-contaminacion-rios-aguas-residuales.html)
- 430 El Comercio (2015b). La Mariscal Sucre, Segundo Puesto En El 'Top Ten' De Las Más
 431 Transitadas De Quito. [http://www.elcomercio.com/actualidad/quito-transito-](http://www.elcomercio.com/actualidad/quito-transito-avmariscalsucre-congestion.html)
 432 [avmariscalsucre-congestion.html](http://www.elcomercio.com/actualidad/quito-transito-avmariscalsucre-congestion.html)
- 433 El Telégrafo (2013). La EPMOP Estabilizará Dos Taludes En Av. Simón Bolívar.
 434 [http://www.eltelegrafo.com.ec/noticias/quito/11/la-epmmop-estabilizara-dos-](http://www.eltelegrafo.com.ec/noticias/quito/11/la-epmmop-estabilizara-dos-taludes-en-av-simon-bolivar)
 435 [taludes-en-av-simon-bolivar](http://www.eltelegrafo.com.ec/noticias/quito/11/la-epmmop-estabilizara-dos-taludes-en-av-simon-bolivar)
- 436 El Universo (2017). Municipio De Quito Destinó Más De 15 Millones De Dólares Para
 437 La Época Invernal.
 438 [http://www.eluniverso.com/noticias/2017/06/11/nota/6227731/municipio-quito-](http://www.eluniverso.com/noticias/2017/06/11/nota/6227731/municipio-quito-destino-mas-15-millones-dolares-epoca-invernal)
 439 [destino-mas-15-millones-dolares-epoca-invernal](http://www.eluniverso.com/noticias/2017/06/11/nota/6227731/municipio-quito-destino-mas-15-millones-dolares-epoca-invernal)
- 440 Falaschi, F., Giacomelli, F., Federici, P., Puccinelli, A., D'Amato Avanzi, G., Pochini,
 441 A. and Ribolini, A. (2009). Logistic regression versus artificial neural networks:



- 442 Landslide susceptibility evaluation in a sample area of the Serchio River valley, Italy.
 443 Natural Hazards, 50, 551-569.
- 444 Feizizadeh, B. and Blaschke, T. (2013). GIS-multicriteria decision analysis for landslide
 445 susceptibility mapping: comparing three methods for the Urmia lake basin,
 446 Iran. Natural hazards, 65(3), 2105-2128.
- 447 Fookes, P., Sweeney, M., Manby, C. and Martin, R. (1985). Geological and geotechnical
 448 engineering aspects of low-cost roads in mountainous terrain. Engineering Geology,
 449 21, 1-152.
- 450 Grahn, T. and Jaldell, H. (2017). Assessment of data availability for the development of
 451 landslide fatality curves. Landslides, 14, 3, 1113–1126.
- 452 Guzzetti, F., Carrara, A., Cardinali, M. and Reichenbach, P. (1999). Landslide hazard
 453 evaluation: a review of current techniques and their application in a multi-scale study,
 454 Central Italy. Geomorphology, 31, 181–216.
- 455 Hervás, J., Barredo, J. and Lomoschitz, A. (2012). Elaboración de mapas de
 456 susceptibilidad de deslizamientos mediante SIG, Teledetección y Métodos de
 457 evaluación multicriterio. Aplicación a la depresión de Tirajana (Gran Canaria).
 458 Instituto Geológico y Minero de España, 169 - 180.
- 459 INIGEMM (Instituto Nacional de Investigación Geológica Minero Metalúrgico) (1978-
 460 1980. Geologic maps in a scale of 1:50000 of: Quito (1978), Sangolquí (1980) and El
 461 Quinche (1980). <http://www.geoinvestigacion.gob.ec/mapas-tematicos-1-50-000/>.
- 462 Isik, Y. (2009). Landslide susceptibility mapping using frequency ratio, logistic
 463 regression, artificial neural networks and their comparison: A case study from Kat
 464 landslides (Tokat—Turkey). Computers & Geosciences, 35, 1125 – 1138.
- 465 Jaramillo Castelo, C.A., Padilla Almeida, O., Cruz D’Howitt, M. and Toulkeridis, T.
 466 (2018). Comparative determination of the probability of landslide occurrences and
 467 susceptibility in central Quito, Ecuador”. 5th International Conference on
 468 eDemocracy and eGovernment, ICEDEG 2018, 136-143.
- 469 Kjellgren, S. (2013). Exploring local risk managers' use of flood hazard maps for risk
 470 communication purposes in Baden-Württemberg. Natural Hazards and Earth System
 471 Sciences, 13, 1857 – 1872.



- 472 Koirala, N. and Watkins, A. (1988). Bulk appraisal of slopes in Hong Kong. In
473 Landslides (ed.C. Bonnard), Balkema, Rotterdam, 2, 1181 - 1186.
- 474 La Hora (2017). Se Declara Emergencia Debido Al Temporal.
475 <https://lahora.com.ec/noticia/1102042279/se-declara-emergencia-debido-al-temporal>
- 476 Lacasse, S., Nadim, F., y Kalsnes, B. (2010). Living with landslide risk. Geotechnical
477 Engineering Journal of the SEAGS & AGSSEA, 41,4: 13pp
- 478 Loarte Merino, G.V. (2013). Determinación de zonas susceptibles a movimientos en
479 masa por factores condicionantes y desencadenantes en la parroquia Lloa, del cantón
480 Quito en la provincia de Pichincha. Unpubl. thesis Universidad San Francisco de
481 Quito, Cumbaya, Ecuador: 100pp
- 482 Malczewski, J. (1996). A GIS- Based Approach To Multiple Criteria Group Decision -
483 Making. International Journal of Geographical Information Systems, 10, 955 – 971.
- 484 Maryam, I. (2011). A comparative study of fuzzy logic approach for landslide
485 susceptibility mapping using GIS: An experience of Karaj dam basin in Iran. Procedia
486 - Social and Behavioral Sciences, 19, 668 - 676.
- 487 Monsalve, G. (2009). Hidrología En La Ingeniería (2da ed.). Alfaomega, Colombia:
488 358pp
- 489 Moreano, M. (2010). La Biografía Secreta De Las Aguas Quiteñas. Ecuador terra
490 incognita, 65: 10-19.
- 491 Pardeshi, S. D., Autade, S. E. and Pardeshi, S. S. (2013). Landslide hazard assessment:
492 recent trends and techniques. Springer Plus, 2(1): 523pp
- 493 Park, S., Choi, C., Kim, B. and Kim, J. (2013). Landslide susceptibility mapping using
494 frequency ratio, analytic hierarchy process, logistic regression, and artificial neural
495 network methods at the Inje area, Korea. Environmental Earth Sciences, 68, 1443 –
496 1464.
- 497 Pradhan, B. (2013). A comparative study on the predictive ability of the decision tree,
498 support vector machine and neuro-fuzzy models in landslide susceptibility mapping
499 using GIS. Computers & Geosciences, 51, 350 – 365.
- 500 Pradhan, B. and Lee, S. (2010). Landslide susceptibility assessment and factor effect
501 analysis: backpropagation artificial neural networks and their comparison with



- 502 frequency ratio and bivariate logistic regression modelling. *Environmental Modelling*
 503 & Software, 25, 747 – 759.
- 504 Prensa Alcaldía de Quito (2017). Municipio Atiende Emergencias Por Deslizamientos.
 505 [http://prensa.quito.gob.ec/index.php?module=Noticias&func=news_user_view&id=](http://prensa.quito.gob.ec/index.php?module=Noticias&func=news_user_view&id=25751&umt=Municipio%20atiende%20emergencias%20por%20deslizamientos)
 506 [25751&umt=Municipio%20atiende%20emergencias%20por%20deslizamientos](http://prensa.quito.gob.ec/index.php?module=Noticias&func=news_user_view&id=25751&umt=Municipio%20atiende%20emergencias%20por%20deslizamientos)
- 507 Rajakumar, R., Sanjeevi, S., Jayaseelan, S., Isakkipandian, G., Edwin, M., Balaji, P. and
 508 Ehanthalingam, G. (2007). Landslide susceptibility mapping in a hilly terrain using
 509 remote sensing and GIS. *Journal of the Indian Society of Remote Sensing*, 35, 31 -
 510 42.
- 511 Reinoso Chisaguano, I. C. (2015). Evaluación Ambiental Del Río Machángara. Unpubl.
 512 Thesis Escuela Politécnica Nacional, Quito, Ecuador: 178pp
- 513 Saro, L., Woo, J. S., Kwan-Young, O. and Moun-Jin, L. (2016). The spatial prediction
 514 of landslide susceptibility applying artificial neural network and logistic regression
 515 models: A case study of Inje, Korea. *Open Geosciences*, 8, 117 - 132.
- 516 Secretaría de Gestión de Riesgos (2016). Incendios Forestales 2016. 111 situation reports
 517 <http://www.gestionderiesgos.gob.ec/informes-incendios-forestales-2016/>.
- 518 Secretaría de Seguridad y Gobernabilidad del DMQ (2015). Atlas De Amenazas
 519 Naturales y Exposición De Infraestructura Del Distrito Metropolitano De Quito (Vol.
 520 Segunda Edición). Quito, Ecuador: 126pp
- 521 Sepúlveda, S. and Petley, D. (2015). Regional trends and controlling factors of fatal
 522 landslides in Latin America and the Caribbean. *Natural Hazard and Earth System*
 523 *Sciences*, 15(8), 1821 - 1833.
- 524 Silvers, K. and Griffiths, J. (2006). Landslide Affecting The Vía Interoceánica, East Of
 525 Quito, Ecuador. IAEG2006 Paper number 234: 8pp
- 526 Singh, A. K. (2010). Bioengineering techniques of slope stabilization and landslide
 527 mitigation. *Disaster Prevention and Management: An International Journal*, 19, 384 -
 528 397.
- 529 Sowers, G. and Royster, D. (1978). Field Investigation. Landslides analysis and control,,
 530 Special report 176, 81-111.



- 531 Toulkeridis, T., Rodríguez, F., Arias Jiménez, N., Simón Baile, D., Salazar Martínez, R.,
 532 Addison, A., Carreón Freyre, D., Mato, F. and Díaz Perez, C. (2016). Causes and
 533 consequences of the sinkhole at El Trébol of Quito, Ecuador – implications for
 534 economic damage and risk assessment. Nat. Hazards Earth Syst. Sci., 16, 2031-2041.
 535 UNESCO - ROSTALC (1982). Guía Metodológica Para La Elaboración Del Balance
 536 Hídrico Para América Del Sur. Montevideo, Uruguay: Oficina Regional de Ciencia y
 537 Tecnología de la UNESCO para América Latina y el Caribe.
 538 [http://www.unesco.org.uy/phi/biblioteca/files/original/4028d09481fd2531c30f5cd66](http://www.unesco.org.uy/phi/biblioteca/files/original/4028d09481fd2531c30f5cd6660298c3.pdf)
 539 [60298c3.pdf](http://www.unesco.org.uy/phi/biblioteca/files/original/4028d09481fd2531c30f5cd6660298c3.pdf).
 540 Velasteguí, V., Reinoso, I. and Valencia, N. (2015). Modelación numérica de la calidad
 541 del agua en ríos mediante el programa computacional HEC-RAS versión 4.0 Caso de
 542 estudio: Río Machángara dentro de la zona de influencia de la Ciudad de Quito. 1er
 543 Congreso Iberoamericano sobre sedimentos y ecología. Queretaro, México: 5pp
 544 Zafrir Vallejo, R., Padilla Almeida, O., Cruz D'Howitt, M., Toulkeridis, T., Rodriguez
 545 Espinosa, F., Mato, F. and Morales Muñoz, B. (2018). Numerical probability
 546 modeling of past, present and future landslide occurrences in northern Quito, Ecuador
 547 – Economic implications and risk assessment”. 5th International Conference on
 548 eDemocracy and eGovernment, ICEDEG 2018, 117-125.